*International Journal of Astrobiology* 15 (2): 119–126 (2016)
doi:10.1017/S1473550415000221 

# An Assessment of macro-scale *in situ* Raman and ultraviolet-induced fluorescence spectroscopy for rapid characterization of frozen peat and ground ice

Janelle R. Laing[1], Hailey C. Robichaud[2] and Edward A. Cloutis[2]

[1]*Department of Environmental Studies and Sciences, University of Winnipeg, 515 Portage Avenue, Winnipeg, Manitoba, Canada R3B 2E9*
[2]*Department of Geography, University of Winnipeg, 515 Portage Avenue, Winnipeg, Manitoba, Canada R3B 2E9*

**Abstract**: The search for life on other planets is an active area of research. Many of the likeliest planetary bodies, such as Europa, Enceladus, and Mars are characterized by cold surface environments and ice-rich terrains. Both Raman and ultraviolet-induced fluorescence (UIF) spectroscopies have been proposed as promising tools for the detection of various kinds of bioindicators in these environments. We examined whether macro-scale Raman and UIF spectroscopy could be applied to the analysis of unprocessed terrestrial frozen peat and clear ground ice samples for detection of bioindicators. It was found that this approach did not provide unambiguous detection of bioindicators, likely for a number of reasons, particularly due to strong broadband induced fluorescence. Other contributing factors may include degradation of organic matter in frozen peat to the point that compound-specific emitted fluorescence or Raman peaks were not resolvable. Our study does not downgrade the utility of either UIF or Raman spectroscopy for astrobiological investigations (which has been demonstrated in previous studies), but does suggest that the choice of instrumentation, operational conditions and sample preparation are important factors in ensuring the success of these techniques.

*Received 27 March 2015, accepted 23 June 2015, first published online 24 August 2015*

**Key words:** astrobiological investigation, bioindicator, biomarker, Raman spectroscopy, spectroscopy, ultraviolet-induced fluorescence.

## Introduction

The ability to detect and characterize or discriminate microorganisms and biomolecules that may exist in cold environments is relevant to a variety of science questions. These include whether life existed or exists on Mars, and how microorganisms may react to changes in the terrestrial global climate. The importance of these questions necessitates the development of analytical techniques that can be applied to address them.

The search for life beyond the Earth is an area of active investigation. A wide array of techniques have been proposed for detecting and characterizing signs of past or present life on other planetary bodies using orbital and landed assets. Mars is currently the planetary body where the search for extant or extinct life is most advanced. Future landed missions, such as the 2018 ExoMars rover and Mars 2020 rover have astrobiology as one of their main science drivers (Mustard *et al*. 2013; European Space Agency 2014).

Among techniques planned or proposed for deployment to Mars to address astrobiology science goals are Raman spectroscopy (Rull *et al*. 2013; Beegle *et al*. 2014; Maurice *et al*. 2015) and ultraviolet-induced fluorescence (UIF) spectroscopy (Beegle *et al*. 2014). The 2018 rover mission to Mars includes a Raman spectrometer as part of the science payload (Böttger *et al*. 2012), with capabilities comparable with the instrument used in this study (i-Raman® System by B&W Tek). Both Raman and UIF spectroscopy have been shown to be capable of detecting the presence of a wide array of bioindicators (e.g., De Gelder *et al*. 2007; Sattler *et al*. 2010; Dartnell *et al*. 2012); (in this paper we use the term 'bioindicators' as shorthand for the range of possible indicators of the presence of past or present life, including biomarkers, biomolecules and live/dead microorganisms). Bioindicators include photosynthetic pigments such as α-chlorophyll and b-chlorophyll, as well as carotenoids such as β-carotene and lycopene. The advantageous characteristics of both Raman and UIF spectroscopy include the ability to conduct stand-off measurements and to acquire usable spectra with no sample preparation.

Raman scattering or the inelastic scattering of photons caused by laser excitation (a 532 nm laser was used in this study), allows for molecular characterization due to transition between energy levels that may be unique for different molecules. Similarly, UIF spectroscopy uses an active incident illumination source (in the case of this study, a 365 nm wavelength ultraviolet (UV) spotlight) and a fibre optic to the directly

reflected and fluorescence-induced light from the sample to the spectrometer.

The Martian surface is currently characterized by low average temperatures, low atmospheric pressure and the possibility of widespread ground ice/permafrost (e.g., Farmer & Doms 1979; Paige 1992; Mellon & Jakosky 1993, 1995; Smith & Zuber 1998; Heldmann *et al.* 2014). Ground ice has been detected at high latitudes (Smith *et al.* 2009), and inferred to be present in mid and high latitudes from orbital observations (Boynton *et al.* 2002; Mitrofanov *et al.* 2002; Byrne *et al.* 2009; Carrozzo *et al.* 2009; Vincendon *et al.* 2010). Thus, any extant Martian life forms are likely to be cryophilic. Additionally the Martian atmosphere has very little available oxygen (0.13%) but has an abundance of $CO_2$ (95.32%) (Rapp 2013), consequently extant life may also be anaerobic. It is also likely that any extant organisms will reside in the subsurface where they are protected from the hostile surface environment and wide swings in diurnal temperatures.

Previous studies have demonstrated the suitability of both Raman and UIF spectroscopy for astrobiology-focused microbiological investigations. While these analytical techniques have been investigated by a number of researchers, best practices for how to optimize their deployment and operation and maximize their science return in a 'real world' Mars setting are not fully resolved (e.g., Groemer *et al.* 2014). For instance, Raman spectroscopic detection of bioindicators in terrestrial analogues of Mars often requires sample pre-processing such as the production of thin sections (Fisk *et al.* 2003), powdering (Edwards *et al.* 2013), culturing, or the use of enhanced (surface enhanced Raman spectroscopy – SERS), confocal and/or microscale techniques (e.g. Serrano *et al.* 2014; Vitek *et al.* 2014). In samples where bioindicator abundances are high enough to be visible (e.g. Antarctic endoliths), Raman spectroscopy can be successfully applied to rocks where the endolith layers have been exposed by fracturing (e.g. Wynn-Williams & Edwards 2000).

Similarly, successful UIF spectroscopy detection of bioindicators is greatly enhanced by pre-processing techniques such as sample staining, sample pre-treatment/preparation, examining a sample at the micro scale (Fisk *et al.* 2003; Storrie-Lombardi & Sattler 2009), or otherwise concentrating any bioindicators. Nevertheless, induced fluorescence techniques can be successfully applied to detection and characterization of different types of bioindicators that naturally exist in cold terrestrial environments (e.g., Bay *et al.* 2005) and Mars-relevant materials (Dartnell *et al.* 2012). Fluorescence imaging can also be combined with Raman spectroscopy to provide more robust detection and characterization of bioindicators (Storrie-Lombardi *et al.* 2001).

The ability of Raman and UIF spectroscopy to detect bioindicators in cold environments and Mars-relevant samples has been demonstrated in a number of studies, indicating that microbial/biomolecule abundances in such terrestrial environments, and other 'extreme' terrestrial environments such as hyperarid deserts (Vitek *et al.* 2014) are sufficient to permit their study by these techniques (e.g., Wynn-Williams & Edwards 2000; Bay *et al.* 2005; Storrie-Lombardi & Sattler 2009; Edwards *et al.* 2013; Serrano *et al.* 2014). Jorge-Villar & Edwards (2006) provided an excellent overview of Raman spectroscopy applications to astrobiology. Additionally, when implemented properly, neither of the above methods damage or compromise the integrity of the samples (Serrano *et al.* 2014) which allows for further manipulation of samples after testing, such as culturing.

The ability to detect the presence of, and characterize, microbes in cold environments is also important for understanding their role in terrestrial carbon cycling, as well as assessing the impacts of warming of these regions on carbon release (Zimov *et al.* 2007; Schuur *et al.* 2009; Schuur & Abbott 2011). Studies of microbial ecosystems in polar terrains have shown that they exist in all types of polar environments (e.g., Price & Sowers 2004; Rohde & Price 2007; Steven *et al.* 2007, 2008; Rohde *et al.* 2008), and that differences exist both in terms of microbial abundances and colony compositions between clear ice, ice wedges and permafrost (Miteva *et al.* 2009; Wilhelm *et al.* 2012). Various properties of microbial communities can be used to infer paleoclimatic conditions. Microbial diversity and abundance is generally highest in the active layer, followed by permafrost, ice wedges and finally ground ice (Steven *et al.* 2008). Viable microorganisms can survive for extended periods of time at subzero temperatures (e.g., Rivkina *et al.* 2005). A number of studies have demonstrated the relevance of polar regions to the search for life on Mars (e.g., Tung *et al.* 2005).

To assist in determining what types of analytical techniques may be most appropriate in searching for extinct or extant life on Mars, we investigated the capabilities of macro-scale Raman and UIF spectroscopy for characterizing untreated frozen peat (supplementary Figure 1) from discontinuous permafrost and clear ice lens samples (supplementary Figure 2). Our goals were to determine whether macro-scale Raman and UIF spectroscopy of samples with no additional treatment (beyond extraction from the field and sterilization of the outer surface) could detect spectroscopic signatures that could be related to bioindicators, and whether differences in Raman and UIF spectra exist between clear ice lenses and frozen peat. Follow-on work is planned to characterize the bioindicators that are present in our samples.

The National Snow and Ice Data Centre defines ground ice as a general term referring to all types of ice contained in freezing and frozen ground and defines peat as a deposit consisting of decayed or partially decayed humified plant remains commonly formed in waterlogged areas where oxygen is absent or present at low levels (van Everdingen 1998). The terms ground ice and clear ice lens are used interchangeably throughout this paper.

## Methodology

### *Study Site*

This study was conducted in the vicinity of the Churchill Northern Studies Centre located near the town of Churchill, Manitoba, Canada. This is a sub-arctic region where

https://doi.org/10.1017/S1473550415000221 Published online by Cambridge University Press

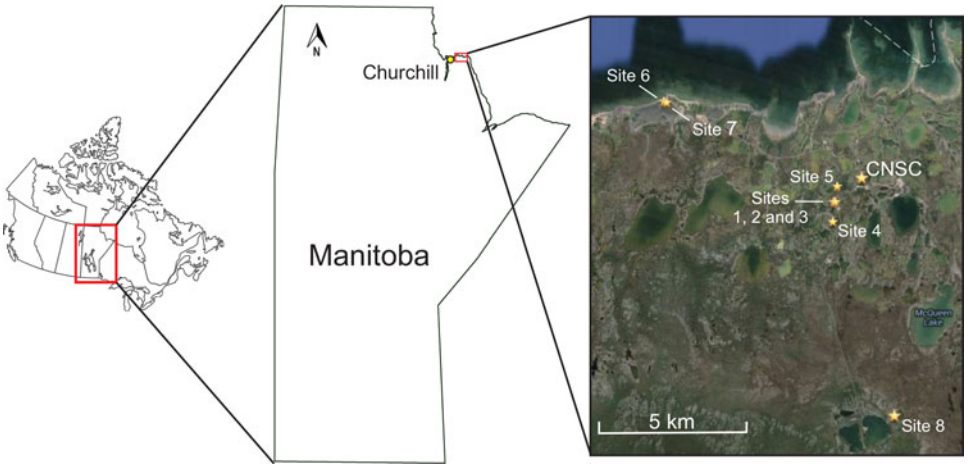


**Fig. 1.** Study region and sample sites 1–8 near Churchill, Manitoba, Canada.

Table 1. *Sample collection time, date and coordinates*

| Time | Latitude | Longitude | Sample ID |
|---|---|---|---|
| 8:40 | N 58.72600 | W 93.84173 | 1–1 |
| | | | 1–2 |
| 9:02 | N 58.72635 | W 93.84037 | 2–1 |
| | | | 2–2 |
| | | | 2–3 |
| 9:13 | N 58.72635 | W 93.84037 | 3–1 |
| | | | 3–2 |
| 10:22 | N 58.73255 | W 93.83920 | 4–1 |
| | | | 4–2 |
| | | | 4–3 |
| | | | 4–4 |
| | | | 4–5 |
| | | | 4–6 |
| 16:00 | N 58.71792 | W 93.84253 | 5–1 |
| | | | 5–2 |
| 16:30 | N 58.76739 | W 93.97609 | 6–1 |
| | | | 6–2 |
| | | | 6–3 |
| 17:00 | N 58.76722 | W 93.97401 | 7–1 |
| 15:30 | N 58.63568 | W 93.98967 | 8–1 |
| | | | 8–2 |

discontinuous permafrost and subsurface clear ground ice are present, making it a suitable analog for research on the microbial composition of ground ice. Sample sites in the Churchill area were chosen based on knowledge of areas containing permafrost or clear ice lenses. Study sites 1, 2 and 3 are located near Strange Lake, site 4 is directly south of sites 1–3 and site 5 is directly north of sites 1–3. Sites 6 and 7 are located on the coast of Hudson Bay, and site 8 is located east of Twin Lakes (Fig. 1, Table 1).

*Sample collection and analysis*

Samples were collected in the field in late August 2014 using a combination of shovels and rock hammers. We sampled both clear ground ice, as well as permafrost that contained variable amounts of rock-derived regolith and partially decayed plant matter (peat). Table 2 describes the nature of the samples. The frozen samples were placed in sterile plastic sample containers and stored in ice in an insulated cooler. The samples were transported to the laboratory within 2 h of collection and placed in a chest freezer maintained at ~−20°C.

For the spectral measurements, one sample at a time was removed from the chest freezer. The samples were handled with sterile nitrile gloves. The frozen peat samples were lightly rinsed with distilled deionized water prior to spectral measurements. Spectral measurements were conducted on fractured surfaces that had not been in contact with the sampling tools. The clear ground ice samples were wiped with isopropyl alcohol cotton swabs and then rinsed with distilled deionized water prior to the spectral measurements. The rationale for this minimal pre-treatment was to remove any contaminants that may have been introduced during sample acquisition, but to otherwise retain the characteristics of samples as they would be encountered in the field. For the spectral measurements, each sample was placed in an aluminium sample boat that was also cleaned with the isopropyl alcohol swabs and distilled deionized water.

*UIF spectra*

We used an Ocean Optics Maya 2000 Pro for measuring the UIF spectra, due to its high resolution (0.42–0.46 nm) and wide spectral range (200–1133 nm). For the UIF measurements we constructed a light-proof enclosure. The samples were illuminated at 45° from normal with a 365 nm UV lamp (UVP Model B-100AP operating at 100 W). The Maya spectrometer was equipped with a fibre optic cable positioned normal to the sample that directed the emitted/reflected light from the sample to the Maya. A dark scan was completed prior to the spectral measurements. The integration time was set to 10 000 ms, and 10 successive scans were averaged to optimize signal to noise. The fibre optic cable was placed ~25 mm from the sample, providing a spot size of ~20 mm.

*Raman spectra*

Raman spectra were acquired with a B&W Tek i-Raman® System. It uses a 532 nm laser for Raman excitation and a

https://doi.org/10.1017/S1473550415000221 Published online by Cambridge University Press

Table 2. *Name and ice type of each sample*

| Site | Sample name | | Sample type (FP = frozen peat; CI = clear ice) |
|---|---|---|---|
| 1 | 1–1 | | FP |
| | Side A | Side B | |
| | 1–2 | | FP |
| | Side A | Side B | |
| 2 | 2–1 | | FP |
| | Side A | Side B | |
| | 2–2 | | FP |
| | Side A | Side B | |
| | 2–3 | | FP |
| | Side A | Side B | |
| 3 | 3–1 | | FP |
| | Side A | Side B | |
| | 3–2 | | FP |
| | Side A | Side B | |
| 4 | 4–1 | | FP |
| | Side A | Side B | |
| | 4–2 | | FP |
| | Side A | Side B | |
| | 4–3 | | FP |
| | Side A | Side B | |
| | 4–4 | | FP |
| | Side A | Side B | |
| | 4–5 | | FP |
| | Side A | Side B | |
| | 4–6 | | FP |
| | Side A | Side B | |
| 5 | 5–1 | | CI |
| | Side A | Side B | |
| | 5–2 | | CI |
| | Side A | Side B | |
| 6 | 6–1 | | CI |
| | Side A | Side B | |
| | 6–2 | | CI |
| | Side A | Side B | |
| | 6–3 | | CI |
| | Side A | Side B | |
| 7 | 7–1 | | CI |
| 8 | 8–1 | | CI |
| | 8–2 | | CI |

fibre optic probe to provide illumination and measure emitted light. A polystyrene block was used to calibrate the instrument before and after sample measurements. A dark scan was acquired before each sample spectrum. Each sample was scanned once with the laser output level set to 100% at integration times ranging from 500 to 20 000 ms. Integration times were varied to optimize signal to noise.

## Results

To ensure that the analysis did not include unexpected contributions from any background materials, Raman and UIF spectra of the aluminium boat and alcohol-infused cotton swab were measured prior to the sample measurements. The UIF spectra exhibit an expected strong emission peak in the 365 nm region, as well as a weaker overtone doublet in the 740–810 nm region

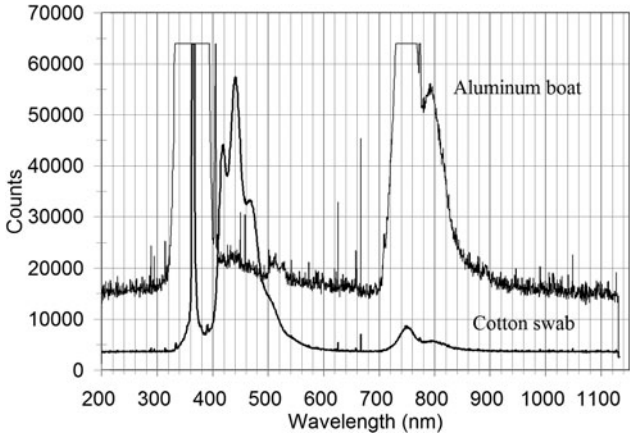


**Fig. 2.** Ultraviolet-induced fluorescence (UIF) spectra of the aluminium boat used to hold samples (thin line) and alcohol-infused cotton swab (thick line).

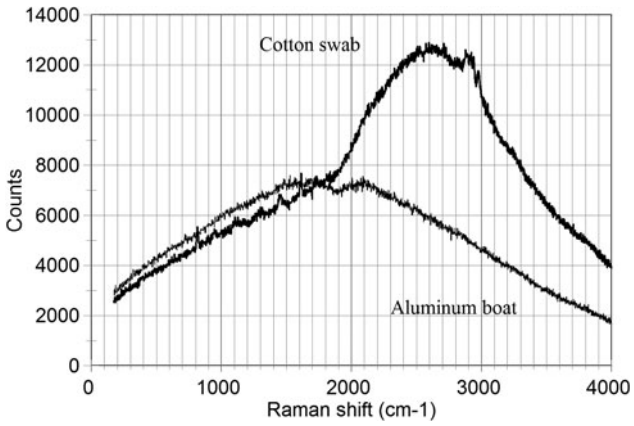


**Fig. 3.** Raman spectra of the aluminium boat used to hold samples (thin line) and alcohol-infused cotton swab (thick line).

from the UV lamp. The cotton swab showed a region of overlapping emission peaks in the ~400–500 nm region attributable to the cotton (Fig. 2) (Gavrilov & Ermolenko 1966). The Raman spectra of the non-sample materials (Fig. 3) show that the aluminium boat exhibits a broad doublet of fluorescence with peaks near 1600 and 2100 $cm^{-1}$, and no discernible Raman peaks (Ponosov & Stretslov 2012). The cotton swab spectrum has a broad peak centred near 2600 $cm^{-1}$ and additional narrow peaks near 2800 and 2950 $cm^{-1}$. There are also a series of weak Raman peaks in the ~1000–2000 $cm^{-1}$ region (Gremlich & Yan 2001).

The illumination conditions for the UIF spectra were such that contributions from the aluminium boat could not be completely removed, particularly for the clear ground ice samples. As a result, we confined our search for UV-induced fluorescence peaks to wavelength regions outside of those attributable to the UV light source and aluminium boat. While the UIF spectra of the frozen peat samples did exhibit evidence of fluorescence, none of the features could be confidently attributed to their organic material (Fig. 4). The most promising wavelength region, 400–450 nm, is also the region where the aluminium

https://doi.org/10.1017/S1473550415000221 Published online by Cambridge University Press

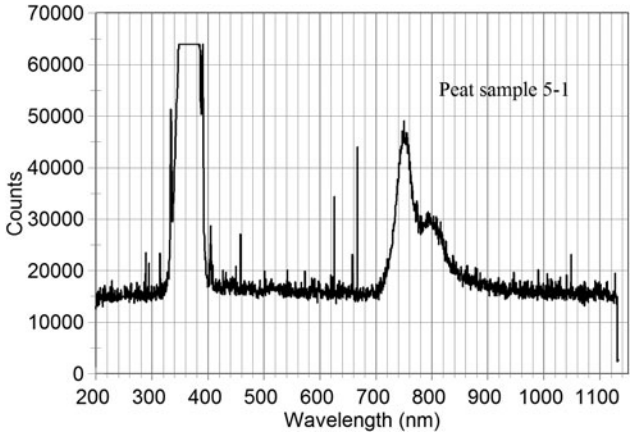


**Fig. 4.** Ultraviolet-induced fluorescence (UIF) spectrum of frozen peat sample 5–1.

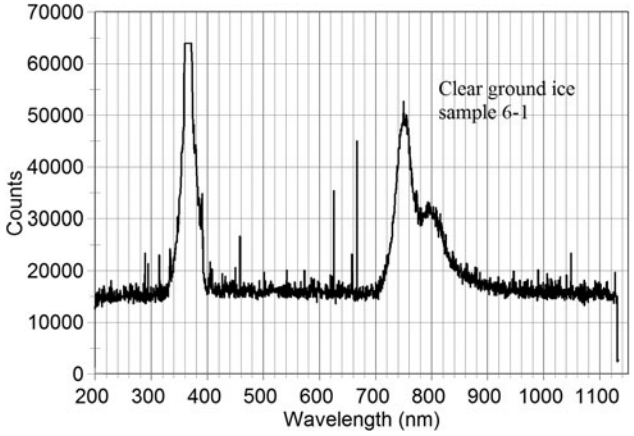


**Fig. 5.** Ultraviolet-induced fluorescence (UIF) spectrum of clear ground ice sample 6–1.

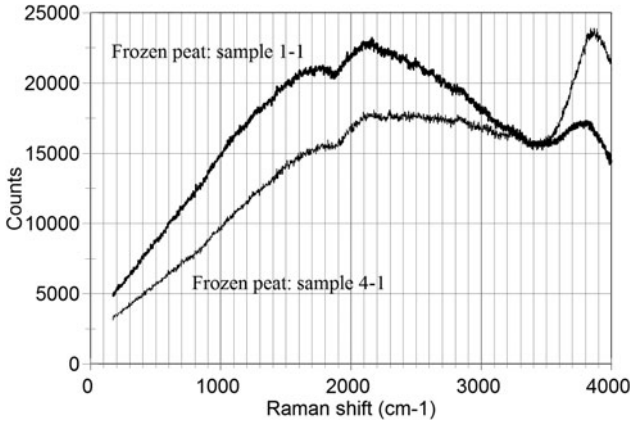


**Fig. 6.** Raman spectra of two frozen peat samples: thick line: sample 1–1; thin line: sample 4–1.

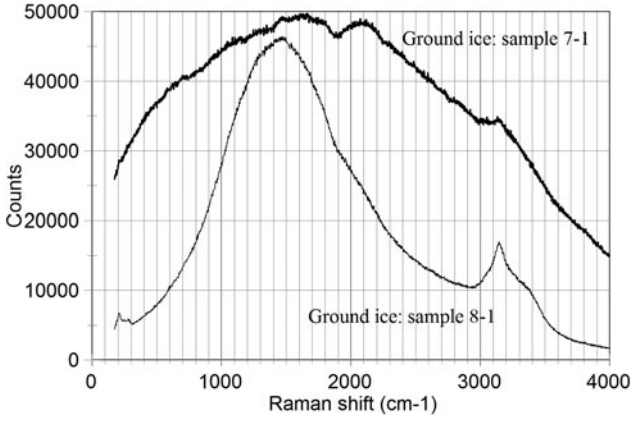


**Fig. 7.** Raman spectra of ground ice samples: thick line: sample 7–1; thin line: sample 8–1.

boat exhibits a broad fluorescence peak. The clear ground ice sample UIF spectra also exhibited this weak 400–450 nm peak as well as an additional peak near 520 nm that is also seen in the UIF spectrum of the aluminium boat (Fig. 5). Once again, the clear ground ice samples did not exhibit any fluorescence features that could confidently be attributed to any embedded organic material.

Raman spectra of major components of peat can be used to interpret the sample spectra. Lignin's most prominent Raman features are as follows: broad peaks in the 1000–1500 $cm^{-1}$ and 3100–3600 $cm^{-1}$ regions, and sharper features near 1650 and 2950 $cm^{-1}$ (Barsberg *et al.* 2005; Gierlinger *et al.* 2012). Raman spectra of cellulose are characterized by broad features near 2900 and 400 $cm^{-1}$, and sharper peaks near 1100 and 1350 $cm^{-1}$ (Schenzel & Fischer 2004). Chlorophyll Raman spectra exhibit a broad rise in emission from 200 to 1000 $cm^{-1}$, and the most prominent sharp Raman peaks are located near 1000, 1300, 1350, 1550, 2950 and 3000 $cm^{-1}$ (e.g., Cai *et al.* 2002). Raman spectra of ice exhibit a broad emission crest in the 3000–3600 $cm^{-1}$ region, with peak near 3170 $cm^{-1}$ and an additional shoulder near 3400 $cm^{-1}$ (Bakker 2004; Park *et al.* 2010). Additional weaker lower-frequency bands can be present near 200 and 300 $cm^{-1}$ (Faure & Chosson 1978), as well as a weak hump near 1600 $cm^{-1}$ (Fukazawa & Mae 2000).

Our Raman sample spectra exhibit some variability and differences between frozen peat and clear ground ice. The frozen peat samples are characterized by a broad fluorescence peak that may mask any organic-specific Raman peaks (Fig. 6). They all exhibit the fluorescence 'absorption band' near 1900 $cm^{-1}$ that can be attributed to the aluminium sample boat. In addition, they have a broad Raman hump near 3800 $cm^{-1}$ and a weaker shoulder near 3400 $cm^{-1}$. These features are likely attributable to some combination of ice and decayed organic matter; more specific assignments are not feasible. There are occasional weaker Raman humps near 2850 $cm^{-1}$ that may be attributable to cellulose/lignin, but this feature is not ubiquitous or strong.

Clear ground ice Raman samples also exhibit some variability (Fig. 7). The aluminium boat absorption band near 2900 $cm^{-1}$ is nearly ubiquitous. The dominance of ice is evident in the sample 8–1 spectrum: it shows weak but resolvable ice peaks near

https://doi.org/10.1017/S1473550415000221 Published online by Cambridge University Press

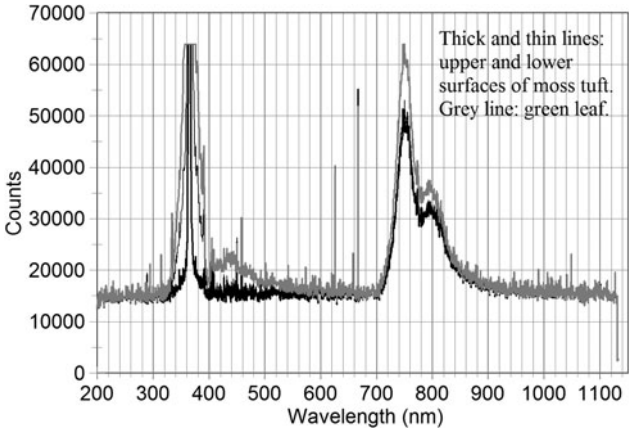


**Fig. 8.** Ultraviolet-induced fluorescence (UIF) spectra of a moss tuft and green leaf.

200 and 300 $cm^{-1}$ and the ice-associated peak and shoulder near 3170 and 3400 $cm^{-1}$. Any organic-associated Raman peaks are not apparent in the clear ground ice sample spectra. In all cases, fluorescence is present.

## Discussion and conclusions

To better understand the spectral properties of our samples, we measured UIF and Raman spectra of various 'extraneous' materials that may contribute to or explain the spectral properties of our samples; such materials included limestone (the dominant contributor to the local regolith), and moss and shrub leaves (as proxies for the biomass contributing to peat formation). The UIF spectra of live moss and green leaves are shown in Fig. 8. The spectra are dominated by reflected light from the UV light source (peaks in the 365 and 740–800 nm region). While the moss spectra do not display any robust additional emission features, the green leaf exhibits an emission feature ranging from ~400 to >500 nm and centred near 440 nm, that can be attributed to various relevant organic compounds such as chlorophyll, polycyclic aromatic hydrocarbons and microbial cells (e.g., Papageorgiou 2004; Bay *et al.* 2005; Dartnell *et al.* 2012). The lack of this feature in our frozen peat samples has a number of possible explanations. Even though these samples contain vegetative matter, it has likely degraded to the point that any UV-active compounds are not present in sufficient abundances to generate a detectable amount of fluorescence in this wavelength region. It is also possible that the peat matrix is sufficiently absorbing that there is not enough interaction of incident UV light with the sample or the sample effectively absorbs any UV-generated visible region photons. It is also possible that the molecular complexity of the vegetative matter results in numerous, but weak, overlapping Raman peaks that collectively result in no discernible Raman peaks. These results also suggest that the mere presence of abundant vegetative matter is insufficient to ensure detection by macro-scale UIF.

To overcome the lack of expected fluorescence, a number of approaches are possible. As mentioned before, sample pre-processing can provide viable UIF detection of organic matter, even when relevant fluorescing substances are present in low concentrations (in extreme environments). Further improvements may be possible by examining samples at the micro-scale and focusing on organic-rich areas. In addition, it is possible that our samples may possess fluorescence features in the 700–900 nm region, and detection of such features was not possible with our current set-up. The use of blocking filters would enable this wavelength region to be more effectively interrogated. Finally, any background materials that may contribute to the spectrum measured by the spectrometer should have minimal or no native fluorescence. It was hoped that the clear ground ice samples would show spectral features indicative of any bioindicators, based on the fact that because the UV light is only weakly absorbed by the ice, it would interact with a large sample volume. However this was not the case either due to low bioindicator abundances (Steven *et al.* 2008) or because of fluorescence interferences from background materials such as the sample holder.

The Raman spectra were generally more effective at providing useful information on the peat and clear ground ice samples. Once again, however, induced fluorescence was present in the spectra, from the samples and/or background materials. As with the UIF spectra, it is likely that the organic matter in the peat samples was either so degraded and/or compositionally complex, that molecule-specific Raman peaks were suppressed by the fluorescence or 'masked' due to multiple overlapping Raman peaks. In the case of the clear ground ice samples, the Raman spectra did display features attributable to the ice, but there was also significant fluorescence. Once again, it appears that bioindicator abundances may have been too low to allow for detection of specific Raman peaks, particularly in light of the substantial induced fluorescence.

One of the goals of our investigation was to determine whether frozen peat would be amenable to characterization by UIF and Raman spectroscopies. However, it appears that our approach (macro-scale, no appreciable sample pre-processing or pre-treatment) is not suitable for interrogating such samples, and we attribute this to appreciable induced fluorescence and possibly to the complexity of the organic matter that results in a 'washing out' of any discrete Raman peaks. In the case of the clear ground ice samples, it was hoped that the large interrogated volume of the sample would overcome presumed low abundances of bioindicators. Again, however, it appears that induced fluorescence, in this case from background materials, was of sufficient magnitude to suppress any material-specific Raman or fluorescence peaks, with the exception of water ice. To improve the utility of Raman spectroscopy for detecting bioindicators in clear ground ice, working at the micro-scale, perhaps combined with fluorescence spectroscopy to identify regions of interest (Storrie-Lombardi *et al.* 2001), would be more effective. Again, ensuring that any background materials that could contribute to the fluorescence background are minimized should be emphasized. The choice of excitation wavelength can also improve suppression of fluorescence (Eshelman *et al.* 2014). Another approach for overcoming fluorescence would be the use of time-resolved

https://doi.org/10.1017/S1473550415000221 Published online by Cambridge University Press

Raman spectroscopy, as Raman excitation and fluorescence lifetimes differ (Skulinova *et al*. 2014).

While macro-scale UIF and Raman spectroscopy would be most easily implemented on a planetary lander, as opposed to micro-scale techniques or requiring sample pre-processing prior to spectral measurements, our results suggest that the simplified approach examined here is unsuitable for detection and characterization of bioindicators in frozen peat (supplementary Figure 1) and clear ground ice (supplementary Figure 2).

## Supplementary materials

For supplementary material for this article, please visit http://journals.cambridge.org/S1473550415000221

## Acknowledgements

We would like to thank the Churchill Northern Studies Center for their hospitality and facilities, the Canada Foundation for Innovation, the Manitoba Research Innovation Fund, the Canadian Space Agency and the University of Winnipeg for supporting the acquisition of the infrastructure used in this study, Matthew Morrison for aid in site selection, and Paul Mann for instrument support and training and assistance in data reduction.

## References

Bakker, R.J. (2004). Raman spectra of fluid and crystal mixtures in the systems $H_2O$, $H_2O$-NaCl and $H_2O$-$MgCl_2$ at low temperatures: applications to fluid inclusion research. *Can. Min*. **42**, 1283–1314.

Barsberg, S., Matousek, P. & Towrie, M. (2005). Structural analysis of lignin by resonance Raman spectroscopy. *Macromol. Biosci*. **5**, 743–752.

Bay, R., Bramall, N. & Price, P.B. (2005). Search for microbes and biogenic compounds in polar ice using fluorescence. In *Life in Ancient Ice*, eds. Castello, J.D. & Rogers, S.O., pp. 268–276. Princeton University Press, Princeton, NJ.

Beegle, L.W. *et al*. (2014). SHERLOC: Scanning habitable environments with Raman and luminescence for organics and chemicals, an investigation for 2020. Lunar and Planetary Science Conf. 45, abstract #2835.

Böttger, U., de Vera, J.P., Fritz, J., Weber, I., Hübers, H.W. & Schulze-Makuch, D. (2012). Optimizing the detection of carotene in cyanobacteria in a martian regolith analogue with a Raman spectrometer for the ExoMars mission. *Planet. Space Sci*. **60**(1), 356–362.

Boynton, W., Feldman, W., Squyres, S., Prettyman, T., Bruckner, J., Evans, L., Reedy, R., Starr, R., Arnold, J. & Drake, D. (2002). Distribution of hydrogen in the near surface of Mars: evidence for subsurface ice deposits. *Science* **297**, 81–85.

Byrne, S., Dundas, C.M., Kennedy, M.R., Mellon, M.T., McEWwan, A.S., Cull, S.C., Dauber, I.J., Shean, D.E., Seelos, K.D. & Murchie, S.L. (2009). Distribution of mid-latitude ground ice on Mars from new impact craters. *Science* **325**, 1674–1676.

Cai, Z.-L., Zeng, H., Chen, M. & Larkum, A.W.D. (2002). Raman spectroscopy of chlorophyll *d* from *Acaryochloris marina*. *Biochimica et Biophysica Acta* **1556**, 89–91.

Carrozzo, F.G., Bellucci, G., Altieri, F., D'Aversa, E. & Bibring, J.-P. (2009). Mapping of water frost and ice at low latitudes on Mars. *Icarus* **203**, 406–420.

Dartnell, L.R., Patel, M.R., Storrie-Lombardi, M.C., Ward, J.M. & Muller, J.-P. (2012). Experimental determination of photostability and fluorescence-based detection of PAHs on the martian surface. *Meteorit. Planet. Sci*. **47**, 806–819.

De Gelder, J., De Gussem, K., Vandenabeele, P. & Moens, L. (2007). Reference database of Raman spectra of biological molecules. *J. Raman Spectrosc*. **38**, 1133–1147.

Edwards, H.G.M., Hutchinson, I.B., Ingley, R., Parnell, J., Vitek, P. & Jehlicka, J. (2013). Raman spectroscopic analysis of geological and biogeological specimens of relevance to the ExoMars mission. *Astrobiology* **13**, 543–549.

Eshelman, E., Daly, M.G., Slater, G., Dietrich, P. & Gravel, J.-F. (2014). Ultraviolet Raman wavelength for the *in-situ* analysis of organic compounds relevant to astrobiology. *Planet. Space Sci*. **93–94**, 65–70.

European Space Agency (2014). ExoMars Mission (2018). http://exploration.esa.int/mars/48088-mission-overview/ (accessed 23 October 2014).

Farmer, C.B. & Doms, P.E. (1979). Global seasonal variation of water vapour on Mars and implications for permafrost. *J. Geophys. Res*. **84**, 2881–2888.

Faure, P. & Chosson, A. (1978). The translational lattice-vibration Raman spectrum of singe-crystal ice Ih. *J. Glaciol*. **21**, 65–72.

Fisk, M.R., Storrie-Lombardi, M.C., Douglas, S., Popa, R., McDonald, G. & Di Meo-Savoie, C. (2003). Evidence of biological activity in Hawaiian subsurface basalts. *Geochem. Geophys. Geosy*. **4**(12). doi:10.1029/2002GC000387.

Fukazawa, H. & Mae, S. (2000). The vibrational spectra of ice Ih and polar ice. In *Physics of Ice Core Records*. ed. Hondoh, T. Hokkaido University Press, Hokkaido, Japan, pp. 25–42.

Gavrilov, M.Z. & Ermolenko, I.N. (1966). A study of cellulose luminescence. *Zhurnal Prikladnoi Spektroscopii* **5**, 762–765.

Gierlinger, N., Keplinger, T. & Harrington, M. (2012). Imaging of plant cell walls by confocal Raman microscopy. *Nat. Protoc*. **7**, 1694–1708.

Gremlich, H.-U. & Yan, B. (2001). *Infrared and Raman Spectroscopy of Biological Materials*. CRC Press, New York, NY.

Groemer, G., Sattler, B., Weisleitner, K., Hunger, L., Kohstall, C., Frisch, A., Josefowicz, M., Meszynski, S., Storrie-Lombardi, M. & the MARS2013 Team (2014). Field trial of a dual-wavelength fluorescent emission (L.I.F.E.) instrument and the Magma White Rover during the MARS2013 Mars Analog Mission. *Astrobiology* **14**, 391–405.

Heldmann, J.L., Schurmeier, L., McKay, C., Davila, A., Stoker, C., Marinova, M. & Wilhelm, M.B. (2014). Midlatitude ice-rich ground on Mars as a target in the search for evidence of life and for *in situ* resource utilization on human missions. *Astrobiology* **14**, 102–118.

Jorge-Villar, S.E. & Edwards, H.G.M. (2006). Raman spectroscopy in astrobiology. *Anal. Bioanal. Chem*. **384**, 100–113.

Maurice, S. *et al*. and the SuperCam Team (2015). Science objectives of the SuperCam instrument for the Mars2020 rover. Lunar and Planetary Science Conf. 46, abstract #2818.

Mellon, M.T. & Jakosky, B.M. (1993). Geographic variations in the thermal and diffusive stability of ground ice on Mars. *J. Geophys. Res*. **98**, 3345–3364.

Mellon, M.T. & Jakosky, B.M. (1995). The distribution and behaviour of martian ground ice during past and present epochs. *J. geophys. Res*. **100**, 11781–11799.

Miteva, V., Teacher, C., Sowres, T. & Brenchley, J. (2009). Comparison of the microbial diversity at different depths of the GISP2 Greenland ice core in relationship to deposition climates. *Environ. Microb*. **11**, 640–656.

Mitrofanov, I.'*et al*. (2002). Maps of subsurface hydrogen from the high energy neutron detector, Mars Odyssey. *Science* **297**, 78–81.

Mustard, J.F. *et al*. (2013). Report of the Mars 2020 Science Definition Team, 154 pp., posted July 2013, by the Mars Exploration Program Analysis Group (MEPAG) at http://mepag.jpl,nasa.gov/reports/MEP/Mars_2020_SDT_Report_Final.pdf.

Paige, D. (1992). The thermal stability of near-surface ground ice on Mars. *Nature* **356**, 43–45.

Papageorgiou, G.C. (Ed.). (2004). *Chlorophyll a Fluorescence: A Signature of Photosynthesis* (Vol. **19**). Springer, Dordretch, The Netherlands, 3, pp. 47–48.

Park, S.-H., Kim, Y.-G., Kim, D., Cheong, H.-D., Choi, W.-S. & Lee, J.-I. (2010). Selecting characteristic Raman wavelengths to distinguish liquid water, water vapour, and ice water. *J. Opt. Soc. Korea* **14**, 209–214.

Ponosov, Y.S. & Stretslov, S.V. (2012). Measurements of Raman scattering by electrons in metals: the effects of electron-phonon coupling. *Phys. Rev. B* **86**, 045138.

Price, P.B. & Sowers, T. (2004). Temperature dependence of metabolic rates for microbial growth, maintenance, and survival. *Proc. Natl. Acad. Sci. U. S. A*. **101**, 4631–4636.

Rapp, D. (2012). *Use of Extraterrestrial Resources for Human Space Missions toMmoon or Mars*. Springer Science & Business Media, Heidelberg, Germany.

Rohde, R.A. & Price, P.B. (2007). Diffusion-controlled metabolism for long-term survival of single isolated microorganisms trapped within ice crystals. *Proc. Natl. Acad. Sci. U. S. A*. **104**, 16592–16597.

Rohde, R.A., Price, P.B., Bay, R.C. & Bramall, N. (2008). *In situ* microbial metabolism as a cause of gas anomalies in ice. *Proc. Natl. Acad. Sci. U. S. A.* **10**, 8667–8867.

Rivkina, E., Laurinavichyus, K. & Gilinchinsky, D.A. (2005). Microbial life below the freezing point within permafrost. In *Life in Ancient Ice*, eds. Castello, J.D. & Rogers, S.O., pp. 106–117. Princeton University Press, Princeton, NJ.

Rull, F., Maurice, S., Diaz, E., Lopez, G., Catala, A. & RLS Team (2013). Raman laser spectrometer (RSL) for ExoMars 2018 rover mission: Current status and science operation mode on powdered samples. Lunar and Planetary Science Conf. 44, abstract #3110.

Sattler, B., Storrie-Lombardi, M.C., Foreman, C.M., Tilg, M. & Psenner, R. (2010). Laser-induced fluorescence emission (LIFE) from Lake Fryxall (Antarctica) cryoconites. *Ann. Glaciol*. **51**, 145–152.

Schenzel, K. & Fischer, S. (2004). Applications of FT Raman spectroscopy for the characterization of cellulose. *Lenzinger Berichte* **83**, 64–70.

Schuur, E.A.G., Vogel, J.G., Krummer, K.C., Lee, H., Sickman, J.O. & Osterkamp, T.E. (2009). The effect of permafrost thaw on old carbon release and net carbon exchange from tundra. *Nature* **459**, 556–559.

Schuur, E.A.G. & Abbott, B. (2011). High risk of permafrost thaw. *Nature* **480**, 32–33.

Serrano, P., Wagner, D., Böttger, U., de Vera, J.P., Lasch, P. & Hermelink, A. (2014). Single-cell analysis of the methanogenic archaeon *Methanosarcina soligelidi* from Siberian permafrost by means of confocal Raman microspectrocopy for astrobiological research. *Planet. Space Sci*. **98**, 191–198.

Skulinova, M. *et al*. (2014). Time-resolved stand-off UV-Raman spectroscopy for planetary exploration. *Planet. Space Sci*. **92**, 88–100.

Smith, P.H., Tamppari, L.K., Arvidson, R.E., Bass, D., Blaney, D., Boynton, W.V., Carswell, A., Catling, D.C., Clark, B.C., Duck, T., DeJong, E., Fisher, D., Goetz, W., Gunnlaugsson, H.P., Hecht, M.H., Hipkin, V., Hoffman, J., Hviid, S.F., Keller, H.U., Kounaves, S.P., Lange, C.F., Lemmon, M.T., Madsen, M.B., Markiewicz, W.J., Marshall, J., McKay, C.P., Mellon, M.T., Ming, D.W., Morris, R.V., Pike, W.T., Renno, N., Staufer, U., Stoker, C., Taylor, P., Whiteway, J. A., & Zent, A.P. (2009). H2O at the Phoenix landing site. *Science* **325** (5936), 58–61.

Smith, D.E. & Zuber, M.T. (1998). The relationship between MOLA northern hemisphere topography and the 6.1-Mbar atmospheric pressure surface of Mars. *Geophys. Res. Lett*. **25**(24), 4397–4400.

Steven, B., Briggs, G., McKay, C.P., Pollard, W.H., Greer, C.W. & Whyte, L.G. (2007). Characterization of the microbial diversity in a permafrost sample from the Canadian high Arctic using culture-dependent and culture-independent methods. *Microb. Ecol*. **59**, 513–523.

Steven, B., Pollard, W.H., Greer, C.W. & Whyte, L.G. (2008). Microbial diversity and activity through a permafrost/ground ice core profile from the Canadian high Arctic. *Environ. Microbiol*. **10**, 3388–3403.

Storrie-Lombardi, M.C., Hug, W.F., McDonald, G.D., Tsapin, A.I. & Nealson, H.K. (2001). Hollow cathode ion lasers for deep ultraviolet Raman spectroscopy and fluorescence imaging. *Rev. Sci. Instrum*. **72**, 4452–4459.

Storrie-Lombardi, M.C. & Sattler, B. (2009). Laser-induced fluorescence emission (LIFE): *in situ* nondestructive detection of microbial life in the ice covers of Antarctic lakes. *Astrobiology* **9**(7), 659–672.

Tung, H.C., Bramall, N.E. & Price, P.B. (2005). Microbial origin of excess methane in glacial ice and implications for life on Mars. *Proc. Natl. Acad. Sci. U. S. A*. **102**, 18292. http://www.jstor.org/stable/4152610.

van Everdingen, R. (ed.) (1998). revised 2005. *Multi-Language Glossary of Permafrost and Related Ground-Ice Terms*. National Snow and Ice Data Center/World Data Center for Glaciology, Boulder, CO.

Vincendon, M., Forget, F. & Mustard, J. (2010). Water ice at low to midlatitudes on Mars. *J. Geophys. Res*. **115**(E10). doi:10.1029/2010JE003594.

Vitek, P., Edwards, H.G.M., Jehlicka, J., Ascaso, C., De Los Rios, A., Valea, S., Jorge-Villar, S.E., Davila, A.F. & Wierzchos, J. (2014). Microbial colonization of halite from the hyper-arid Atacama Desert studied by Raman spectroscopy. *Phil. Trans. R. Soc. A* **368**, 3205–3221.

Wilhelm, R.C., Radtke, K.J., Mykytczuk, N.C.S., Greer, C.W. & Whyte, L.G. (2012). Life at the wedge: the activity and diversity of Arctic ice wedge microbial communities. *Astrobiology* **12**, 347–360.

Wynn-Williams, D.D. & Edwards, H.G.M. (2000). Proximal analysis of regolith habitats and protective biomolecules *in situ* by laser Raman spectroscopy: overview of terrestrial Antarctic habitats and Mars analogs. *Icarus* **144**, 486–503.

Zimov, S.A., Schuur, E.A.G. & Chapin, F.S. III (2007). Permafrost and the global carbon budget. *Science* **312**, 1612–1613.